

Received September 7, 2019, accepted September 16, 2019, date of publication September 27, 2019, date of current version October 15, 2019.

Digital Object Identifier 10.1109/ACCESS.2019.2944173

A Fast Linearized Alternating Minimization Algorithm for Constrained High-Order Total Variation Regularized Compressive Sensing

BINBIN HAO¹, JICHAO WANG¹, AND JIANGUANG ZHU^{1,2}

¹College of Science, China University of Petroleum, Qingdao 266580, China

²College of Mathematics and Systems Science, Shandong University of Science and Technology, Qingdao 266590, China

Corresponding author: Jianguang Zhu (jgzhu980@163.com)

This work was supported in part by the National Key Research and Development Program of China under Grant 2017YFC1405600, in part by the Fundamental Research Funds for the Central Universities under Grant 19CX05003A-2, in part by the Training Program of the Major Research Plan of National Science Foundation of China under Grant 91746104, in part by the National Science Foundation of China under Grant 61101208 and Grant 61976126, in part by the Qingdao Postdoctoral Science Foundation under Grant 2016114, in part by the Project of Shandong Province Higher Educational Science and Technology Program under Grant J17KA166, and in part by the Shandong Provincial Natural Science Foundation under Grant ZR2019QA017 and Grant ZR2019MF003.

ABSTRACT In this paper, we propose a new high-order total variation regularized model with box constraint for image compressive sensing reconstruction. Because of the separable structure of this model, we can easily decompose into three subproblems by splitting the augmented Lagrangian function. To effectively solve the proposed new model, a fast alternating minimization method with accelerated technique is presented. Moreover, the proposed method applies a linearized strategy for quadratic terms to get the closed-form solution and reduce the computation cost. Numerical experiments show that our proposed model can get better performance than several current state-of-the-art methods in terms of signal to noise ratio (SNR) and visual perception.

INDEX TERMS Compressive sensing, second-order total variation, alternating direction method, image reconstruction.


I. INTRODUCTION

Recently, compressive sensing as an emerging methodology in digital signal processing was proposed by Donoho [1], Candés *et al.* [2], and Romberg [3] and has drawn extensive attentions from different research fields. The compressive sensing theory demonstrates that sparse signal/image reconstruction can be achieved with only a few or incomplete measurements. Considering its powerful handling capacity, compressive sensing theory has come into use for sensing image processing, magnetic resonance imaging [4]–[7].

In compressive sensing, the sensing procedure for an image $u \in \mathbb{R}^{n^2}$ can be represented as

$$f = Au + \eta. \quad (1)$$

where $u \in \mathbb{R}^{n^2}$ is an original $n \times n$ image, $f \in \mathbb{R}^m$ is the measurement image, $A \in \mathbb{R}^{m \times n^2}$ ($m \ll n^2$) is a sensing matrix, $\eta \in \mathbb{R}^m$ is an additive noise, In this paper, we consider A is a

The associate editor coordinating the review of this manuscript and approving it for publication was Hengyong Yu .

random Gaussian matrix. For problem (1), recovering u from f is an ill-posed problem. The classical least squares approximation can not be adopted directly. In order to overcome the ill-condition of the problem, the idea of regularization is proposed. Among the regularizations, the total variation (TV) regularization is popular and powerful, which is firstly introduced by Rudin *et al.* [8]. The most widely studied TV model for image restoration (in this case $A \in \mathbb{R}^{n^2 \times n^2}$) has the following form:

$$\min_u \frac{\beta}{2} \|Au - f\|^2 + \sum_{i=1}^{n^2} \|\nabla u_i\|, \quad (2)$$

where, ∇ is a gradient operator, $\nabla u_i = (\nabla^x u_i, \nabla^y u_i)^T$ ($i = 1, 2, \dots, n^2$). ∇u_i refers to the discrete gradient of u at the i pixel, $\beta > 0$ is a parameter.

As well known, TV regularization model can preserve sharp edges very well. A number of efficient and robust methods are proposed to solve the TV model. The numerical methods in this literature include such as the Newton

method, gradient projection method, partial differential equation (PDE) based method, alternating minimization method, see for instance, [9]–[16] and references therein. The alternating direction method of multipliers (ADMM) algorithm has been studied extensively [17]–[19], and has been widely used in optimization problems that arise in image processing [20]–[22]. Using the splitting and quadratic penalty techniques, Wang *et al.* [14] proposed an efficient alternating minimization method (FTVd) to solve the problem (2). In [14], the authors show that the FTVd is very efficient. Based on the split and penalty techniques, Xiao and Yang [16] extend the FTVd to the case of recovering images from random projections. Since A is random projection matrix in [16], the computational burden of using the above method to solve the problem will be costly. To avoid this situation, the authors use the linear expansion technique to propose a new alternating minimization algorithm (FTVCS) to solve model (2). Recently, Xiao and Song [23] propose an inexact alternating directions method for total variation regularized compressive sensing problem with linear constraints, and illustrate that the proposed method is effective and promising.

Compressed sensing usually recover a sparse signal by solving an l_1 -norm minimization problem, such as Osher *et al.* [24] extend the Bregman iterative algorithm to solve an l_1 minimization problem in compressed sensing, Figueiredo *et al.* [25] transform the l_1 minimization problem into bound-constrained quadratic program, and propose a gradient projection method to solve compressed sensing problem. However, recent research shows that the reconstruction of a medical image from its partial Fourier samples, nonsmooth regularizations such as the TV regularization is more powerful choices [26]. Although, TV regularization can preserves the edges very well, which also gives rise to some undesired effects and transforms smooth signal into piecewise constant, the so-called staircase effects. In order to eliminate the staircase effects while preserving the edges well in the restored image, some high-order variational models [27]–[31] are introduced, which include the second order TV regularization terms. Compared with the first-order total variation model, the second-order total variation model can remove the staircase effects and preserve the edges well in the process of image restoration.

On the other hand, based on physical significance of the image represents, image value is often non-negative and also has to lie in a certain dynamic range $[p, q]$. For example, for 8 bit images, its pixel range is $[p, q] = [0, 255]$. If the pixel values exceed this range, it will affect the recovery effect of the image. Several studies have shown that imposing bounded constraints on image values can improve the quality of restoration results [32], [33]. Therefore, in the process of image processing, it is necessary to add a constraint to the image to make the pixel values always within a certain range.

As far as we know, few of works have been done to constrained high-order TV compressive sensing problem. Motivated by the above mentions, in this paper, we propose the following box-constraint high-order total variation

minimization model:

$$\min_{u \in \Omega} \frac{\beta}{2} \|Au - f\|^2 + \sum_i \|\nabla^2 u_i\| \quad (3)$$

where, $\Omega = \{u \in R^{n^2} : p \leq u_i \leq q, i = 1, \dots, n^2\}$, $A \in R^{m \times n^2} (m \ll n^2)$, $\sum_i \|\nabla^2 u_i\|$ is the second-order TV norm of u . The definition of the second-order TV norm is similar to the first-order TV norm. The second-order TV norm can be defined by

$$\nabla^2 u_i = \left(\nabla_{x,x} u_i, \nabla_{x,y} u_i, \nabla_{y,x} u_i, \nabla_{y,y} u_i \right),$$

$$\|\nabla^2 u_i\| = \sum_{1 \leq i \leq n^2} \sqrt{|\nabla_{x,x} u_i|^2 + |\nabla_{x,y} u_i|^2 + |\nabla_{y,x} u_i|^2 + |\nabla_{y,y} u_i|^2},$$

here, $\nabla_{x,x} u_i, \nabla_{x,y} u_i, \nabla_{y,x} u_i, \nabla_{y,y} u_i$ refers to the second-order discrete gradient of u at the i pixel. More details about the second order difference refers to [29]. In this paper, instead of solving the model (3) directly, we first introduce two auxiliary variables to transform the constrained minimization problem into the unconstrained problem by using the variable splitting method. Secondly, based on linearized and accelerated strategy, we proposed a fast alternating minimization algorithm to solve the resulting optimization problem. Numerical results demonstrate the proposed algorithm is efficient. Our algorithm performs better than several current state-of-the-art numerical algorithms.

The rest of this paper is organized as follows. In section 2, based on the linearized and accelerated techniques, we propose a fast algorithm to solve the constrained high-order TV compressive sensing problem. In section 3, numerical comparisons with existing methods are carried out to confirm the effectiveness of our proposed method. Finally, concluding remarks are given in section 4.

II. THE PROPOSED ACCELERATING LINEARIZED ALTERNATING MINIMIZATION ALGORITHM

In this section, we describe the proposed fast linearized alternating minimization algorithm for solving the problem (3). Firstly, introducing two auxiliary variables ω and z , the problem (3) can be transformed into the following equivalent constraint problem:

$$\min_{z \in \Omega, u} \frac{\beta}{2} \|Au - f\|^2 + \sum_i \|\omega_i\|$$

$$s.t. \omega_i = \nabla^2 u_i, \quad i = 1, \dots, n^2,$$

$$z = u. \quad (4)$$

Next, we define the augmented Lagrangian of the problem (4) as follows:

$$L(\omega, u, z, \lambda) = \sum_{i=1}^{n^2} (\|\omega_i\| + \frac{\beta_1}{2} \|\omega_i - \nabla^2 u_i\|^2) + \frac{\beta}{2} \|Au - f\|^2$$

$$- \lambda^T (z - u) + \frac{\beta_2}{2} \|z - u\|^2, \quad (5)$$

where, $\beta_1, \beta_2 > 0$ is penalty parameters, $\lambda \in R^{n^2}$ is Lagrange multiplier. The above augmented Lagrangian function combines both the quadratic penalty function and Lagrangian function, which can get more reconstruction accuracy. The iterative formula is generated by the alternate direction method as follows:

$$\begin{cases} \omega^{k+1} = \arg \min_{\omega} L(\omega, u^k, z^k, \lambda^k) \\ u^{k+1} = \arg \min_u L(\omega^{k+1}, u, z^k, \lambda^k) \\ z^{k+1} = \arg \min_z L(\omega^{k+1}, u^{k+1}, z, \lambda^k) \\ \lambda^{k+1} = \lambda^k - \gamma \beta_2 (z^{k+1} - u^{k+1}) \end{cases}$$

In what follows, we solve the above mentioned three subproblems one by one. Firstly, fixed u^k, z^k, λ^k , the minimization of (5) with respect to ω is equivalent to

$$\begin{aligned} \omega^{k+1} &= \arg \min_{\omega} L(\omega, u^k, z^k, \lambda^k) \\ &= \arg \min_{\omega} \sum_{i=1}^{n^2} (\|\omega_i\| + \frac{\beta_1}{2} \|\omega_i - \nabla^2 u_i^k\|^2). \end{aligned} \quad (6)$$

The minimizer of (6) can be obtained by the following two-dimensional shrinkage operator

$$\omega_i^{k+1} = \max\left\{\|\nabla^2 u_i^k\| - \frac{1}{\beta}\right\} \frac{\nabla^2 u_i^k}{\|\nabla^2 u_i^k\|}, \quad i = 1, \dots, n^2.$$

Recently, various acceleration techniques of iterative algorithms are proposed [34]–[38]. For this subproblem, in order to accelerate the convergence of the above mentioned iteration, we employ the acceleration technique in [38] to solve it. In this method, we let

$$\bar{\omega}_i^{k+1} = \max\left\{\|\nabla^2 u_i^k\| - \frac{1}{\beta}\right\} \frac{\nabla^2 u_i^k}{\|\nabla^2 u_i^k\|}, \quad i = 1, \dots, n^2. \quad (7)$$

Then, ω^{k+1} is updated again as follows:

$$\omega^{k+1} = \bar{\omega}^{k+1} + \left(\frac{t_k - 1}{t_{k+1}}\right)(\bar{\omega}^{k+1} - \bar{\omega}^k), \quad (8)$$

where, $t_0 = 1, t_{k+1} = \frac{1 + \sqrt{1 + 4t_k^2}}{2}, \frac{t_k - 1}{t_{k+1}} \in [0, 1]$ is the step length.

Secondly, fixed $\omega^{k+1}, z^k, \lambda^k$, the u subproblem can be written as

$$\begin{aligned} u^{k+1} &= \arg \min_u \frac{\beta_1}{2} \sum_{i=1}^{n^2} \|\omega_i^{k+1} - \nabla^2 u_i\|^2 + \frac{\beta}{2} \|Au - f\|^2 \\ &\quad + \frac{\beta_2}{2} \|z^k - (u + \frac{\lambda^k}{\beta_2})\|^2. \end{aligned} \quad (9)$$

According to the optimal conditions, the minimization problem (9) can be solved by the following equation:

$$\begin{aligned} (\beta A^T A + \beta_1 \nabla^{2T} \nabla^2 + \beta_2 I)u &= \beta A^T f + \beta_1 \nabla^{2T} \omega^{k+1} \\ &\quad - \lambda^k + \beta_2 z^k. \end{aligned} \quad (10)$$

Because A is a random Gaussian matrix, $A^T A$ does not have circulant structure and can't be diagonalized directly. So, it is

extremely heavy to find the exact solution of (10). In order to get the closed-form solutions and reduce the computation cost, we use a linearized strategy for the quadratic term $\frac{1}{2} \|Au - f\|^2$. We linearize $\frac{1}{2} \|Au - f\|^2$ at the current u^k , and the quadratic term can be approximated by

$$\begin{aligned} \frac{1}{2} \|Au - f\|^2 &\approx \frac{1}{2} \|Au^k - f\|^2 + g_k^T (u - u^k) \\ &\quad + \frac{1}{2\tau} \|u - u^k\|^2, \end{aligned} \quad (11)$$

where, $g_k = A^T (Au^k - f)$ is the gradient of $\frac{1}{2} \|Au - f\|^2$ at u^k , $\tau > 0$ is a proximal parameter. Using (11) into (9), then, the formula (9) can be approximately simplified to the following minimization problem:

$$\begin{aligned} u^{k+1} &= \arg \min_u \frac{\beta_1}{2} \sum_{i=1}^{n^2} \|\omega_i^{k+1} - \nabla^2 u_i\|^2 + \beta \left(g_k^T (u - u^k) \right. \\ &\quad \left. + \frac{1}{2\tau} \|u - u^k\|^2 \right) - \lambda^{kT} (z^k - u) + \frac{\beta_2}{2} \|z^k - u\|^2 \\ &= \arg \min_u \frac{\beta_1}{2} \sum_{i=1}^{n^2} \|\omega_i^{k+1} - \nabla^2 u_i\|^2 + \frac{1}{\beta\tau} \|u - (u^k - \tau g_k)\|^2 \\ &\quad - \frac{\beta_2}{2} \|z^k - (u + \frac{\lambda^k}{\beta_2})\|^2 \end{aligned} \quad (12)$$

By solving the above optimization problem, the closed form solution for u^{k+1} can be obtained from the following equation:

$$\begin{aligned} \left(\frac{\beta}{\tau} I + \beta_1 \nabla^{2T} \nabla^2 + \beta_2 I\right)u &= \frac{\beta}{\tau} (u^k - \tau g_k) + \beta_1 \nabla^{2T} \omega^{k+1} \\ &\quad - \lambda^k + \beta_2 z^k. \end{aligned} \quad (13)$$

Under the periodic boundary condition, the coefficient matrix in (13) can be diagonalized by fast Fourier transforms (FFTs). So, the solution of (13) can be obtained by the two FFTs(including one inverse FFT).

Thirdly, for given $\omega^{k+1}, u^{k+1}, \lambda^k$, the minimizer z^{k+1} of problem (5) with respect to z is given by

$$\begin{aligned} z^{k+1} &= \arg \min_{z \in \Omega} -\lambda^T (z - u^{k+1}) + \frac{\beta_2}{2} \|z - u^{k+1}\|^2 \\ &= \arg \min_{z \in \Omega} \|z - (u^{k+1} + \frac{\lambda^k}{\beta_2})\|^2. \end{aligned} \quad (14)$$

Therefore, we can easily get

$$z^{k+1} = P_{\Omega}(u^{k+1} + \frac{\lambda^k}{\beta_2}), \quad (15)$$

where, $P_{\Omega}(\cdot)$ is the projection operator, representing an orthogonal projection onto Ω .

Finally, we update the Lagrange multiplier λ as follows:

$$\lambda^{k+1} = \lambda^k - \gamma \beta_2 (z^{k+1} - u^{k+1}).$$

The full steps of proposed algorithm is summarized as follows:

Algorithm 1 Proposed Algorithm

1. Input: $f, A, \gamma, \beta > 0, \beta_1 > 0, \beta_2 > 0, \tau > 0$ and λ^0
2. Initialization: $u^0 = f, \omega^0 = \nabla^2 u^0, t_0 = 1, \lambda = \lambda^0$
3. **While** “not converged”, **Do**
4. Compute $\bar{\omega}^{k+1}$

$$\bar{\omega}_i^{k+1} = \max \left\{ \|\nabla^2 u_i^k\| - \frac{1}{\beta} \right\} \frac{\nabla^2 u_i^k}{\|\nabla^2 u_i^k\|}, i = 1, \dots, n^2.$$
5. Compute ω^{k+1}

$$t_{k+1} = \frac{1 + \sqrt{1 + 4t_k^2}}{2},$$

$$\omega^{k+1} = \bar{\omega}^{k+1} + \left(\frac{t_k - 1}{t_{k+1}}\right)(\bar{\omega}^{k+1} - \bar{\omega}^k);$$
6. Compute u^{k+1}

$$u^{k+1} = \left(\frac{\beta}{\tau}I + \beta_1 \nabla^{2T} \nabla^2 + \beta_2 I\right)^{-1} \left(\frac{\beta}{\tau}(u^k - \tau g_k) + \beta_1 \nabla^{2T} \omega^{k+1} - \lambda^k + \beta_2 z^k\right);$$
7. Compute z^{k+1}

$$z^{k+1} = P_{\Omega}(u^{k+1} + \frac{\lambda^k}{\beta_2});$$
8. Update λ^{k+1}

$$\lambda^{k+1} = \lambda^k - \gamma \beta_2 (z^{k+1} - u^{k+1}).$$
9. **End Do**
10. Output u^{k+1}

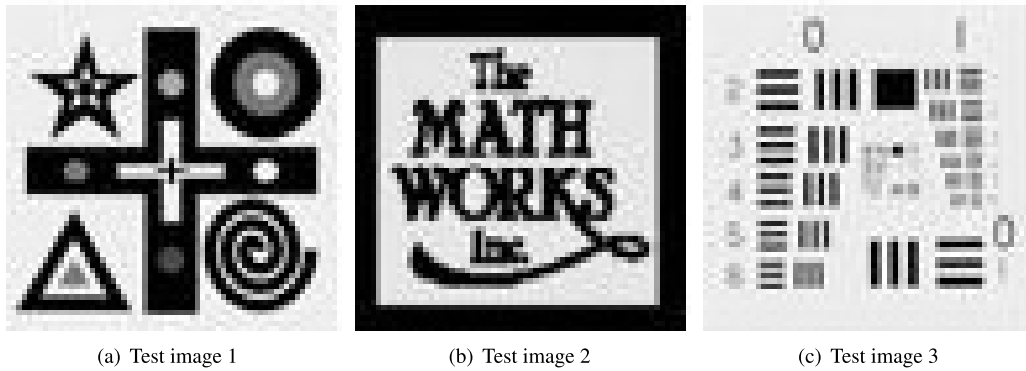


FIGURE 1. Test images.

III. NUMERICAL EXPERIMENTS

In this section, some experimental results are given to show the performance of our proposed method for image reconstruction problems. We perform our algorithm on some different images with Gauss random projection matrix, and compare it with two state-of-the-art algorithms: FTVCS [16] and IADPM [22]. All experiments are performed under Windows 7 and MATLAB 2012a running on a desktop with an core i5 Duo central processing unit at 2.50 GHz and 4 GB memory.

In the following experiments, we use the similar strategy in FTVCS [16], a continuation scheme on β_1 is carried out with $\beta_1 = (2^4, 2^5, 2^6, 2^7)$. The parameters β, β_2 and τ in our proposed method are fixed to be 300, 1.5 and 1.618, respectively. The parameters in FTVCS [16] and IADPM [22] have been recommended. Additionally, in what follows, three different methods were terminated when the relative change less than 10^{-3} , i.e.,

$$\frac{\|u^{k+1} - u^k\|}{\|u^k\|} \leq 1 \times 10^{-3}.$$

The quality of the reconstructed image is evaluated by the relative errors (Rerr), the signal to noise ratio (SNR), which are defined as:

$$Rerr = \frac{\|u - u^0\|}{\|u^0\|} \times 100\%,$$

$$SNR = 10 \log_{10} \frac{\|u^0 - \bar{u}\|^2}{\|u^0 - u\|^2},$$

where u^0, u are the ideal image and the restored image respectively, \bar{u} is the mean intensity value of u^0 . Generally, the larger the SNR values show that the restored images are better.

A. EXPERIMENT 1

In this experiment, the elements of Gauss random matrix $A \in R^{m \times n^2}$ are generated from normal distributions $N(0, 1)$ by `randn(m, n^2)` in MATLAB. The sampling rate of the tested images is defined as $SR = m/n^2$. Owing to storage limitation, the size of the tested image is limited to 64×64 . Besides, we added a zero-mean Gaussian noise with variance σ^2 to three tested images, which are shown in Fig 1. We first apply

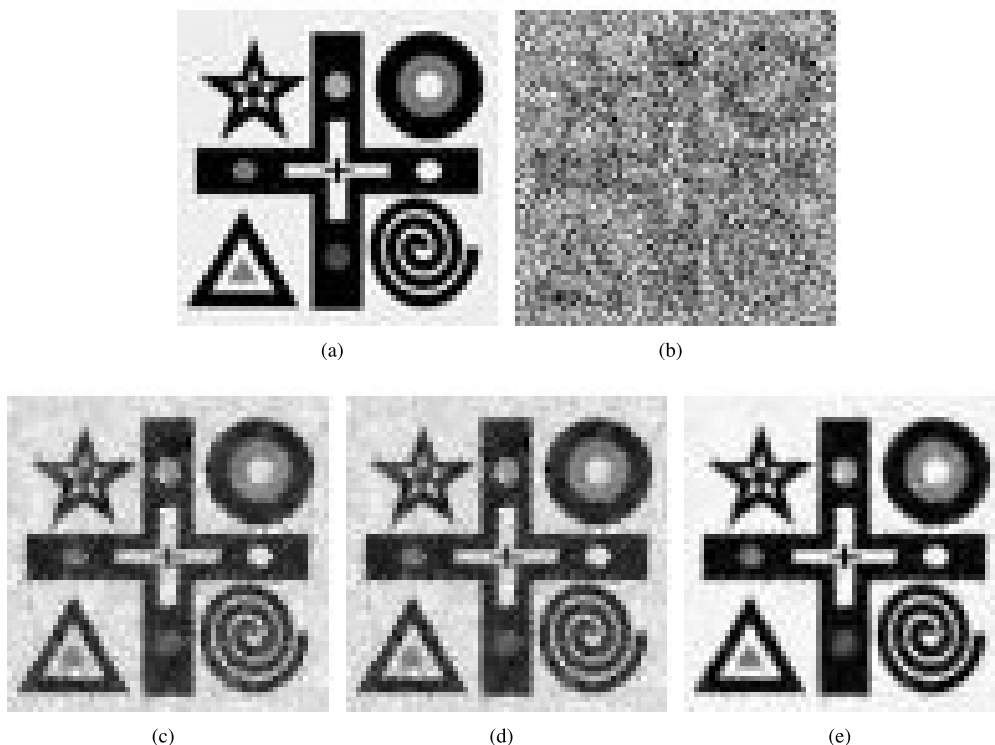


FIGURE 2. (a) The original image; (b) The image with $SR = 50\%$, $\sigma = 0.01$; (c) Reconstructed image by FTVCS; (d) Reconstructed image by IADPM; (e) Reconstructed image by our proposed method.

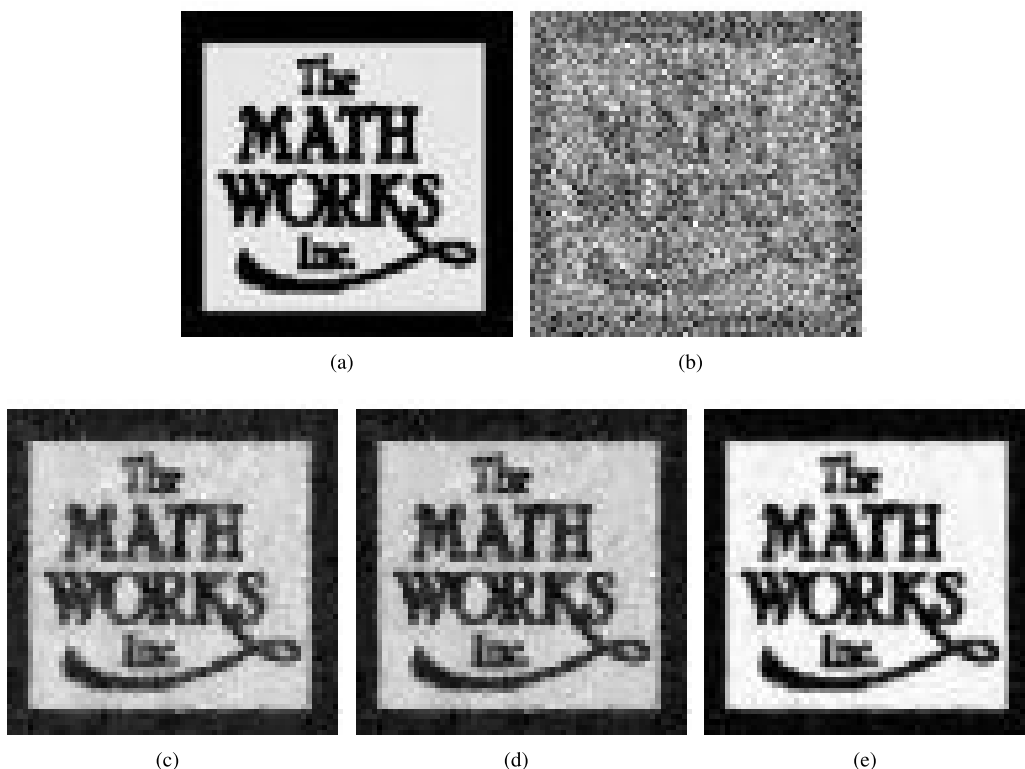


FIGURE 3. (a) The original image; (b) The image with $SR = 50\%$, $\sigma = 0.01$; (c) Reconstructed image by FTVCS; (d) Reconstructed image by IADPM; (e) Reconstructed image by our proposed method.

FTVCS, IADPM and our proposed method to reconstruct three test images with sample ratios $SR = 50\%$ and level of noise $\sigma = 0.01$. The reconstruction results of three test

images are shown in Figs. 2, 3 and 4, respectively. As can be seen from Figs. 2, 3 and 4, the images reconstructed by our proposed method are much closer to the original images

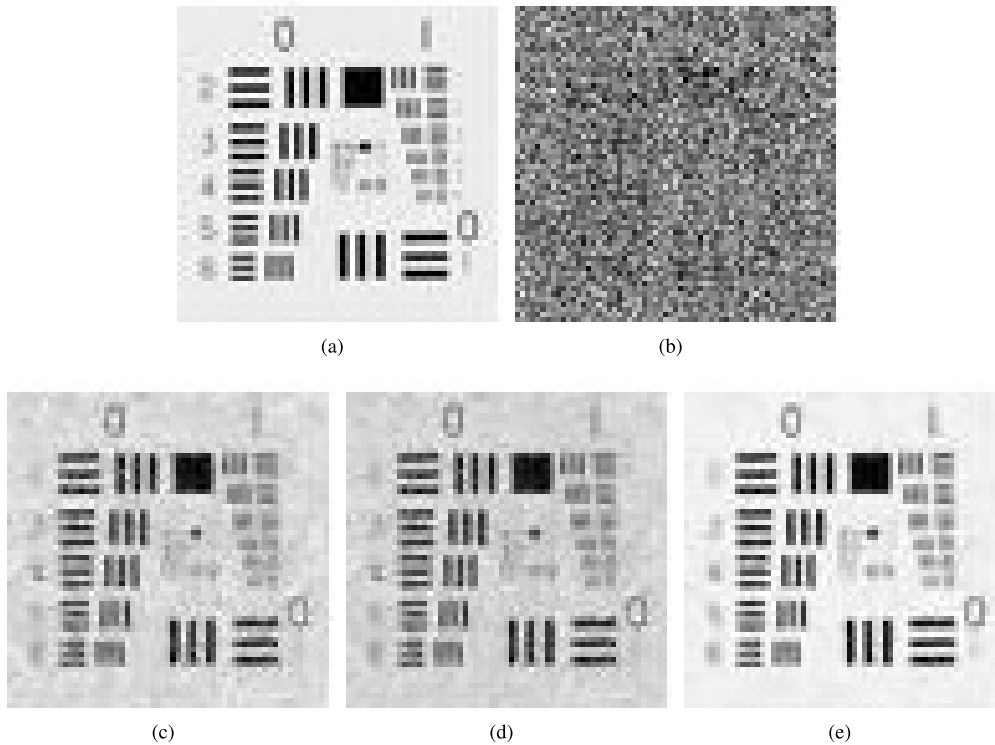


FIGURE 4. (a)The original image; (b) The image with $SR = 50\%$, $\sigma = 0.01$; (c) Reconstructed image by FTVCS; (d) Reconstructed image by IADPM; (e) Reconstructed image by our proposed method.

TABLE 1. The reconstructed results by Our method, FTVCS [16] and IADPM [22] for Test image 1.

Noise Level	SR	Method	Rerr(%)	Time(s)	SNR(dB)
$\sigma = 0.1\%$	30%	FTVCS	21.61%	2.90	18.13
		IADPM	20.72%	1.97	18.53
		Our method	14.24%	1.75	19.66
	40%	FTVCS	16.57%	2.90	20.39
		IADPM	15.02%	2.03	21.27
		Our method	9.62%	1.90	23.18
	50%	FTVCS	11.41%	2.89	22.86
		IADPM	10.32%	2.25	23.68
		Our method	6.41%	1.90	26.66
$\sigma = 1\%$	30%	FTVCS	21.67%	2.86	18.07
		IADPM	20.80%	1.81	18.51
		Our method	14.33%	1.87	19.59
	40%	FTVCS	16.63%	2.89	20.34
		IADPM	15.10%	2.00	21.25
		Our method	9.65%	1.90	23.15
	50%	FTVCS	11.54%	2.82	22.63
		IADPM	10.54%	2.25	23.46
		Our method	6.64%	1.92	26.39

compared with FTVCS and IADPM. These facts indicate that the proposed method has the competitive performance than those of the FTVCS and the IADPM for image reconstruction.

For further show that the benefits of the proposed method, we compare our proposed method with FTVCS, IADPM to reconstruct three test images under different levels of sample ratios $SR = 30\%$, 40% , 50% and different levels of noise $\sigma = 0.1\%$, 1% . The corresponding results including SNR, Rerr and Time are described in Tables 1, 2 and 3, respectively. From the Tables, we can see that, with increasing

TABLE 2. The reconstructed results by Our method, FTVCS [16] and IADPM [22] for Test image 2.

Noise Level	SR	Method	Rerr(%)	Time(s)	SNR(dB)
$\sigma = 0.1\%$	30%	FTVCS	23.45%	2.73	18.55
		IADPM	22.11%	1.76	19.28
		Our method	15.75%	1.93	19.68
	40%	FTVCS	16.59%	2.79	20.89
		IADPM	15.13%	1.97	21.82
		Our method	10.46%	1.90	23.35
	50%	FTVCS	11.78%	2.68	23.61
		IADPM	10.56%	2.26	24.76
		Our method	6.61%	2.03	27.28
$\sigma = 1\%$	30%	FTVCS	23.46%	2.76	18.59
		IADPM	22.10%	1.78	19.38
		Our method	15.75%	1.92	19.67
	40%	FTVCS	16.72%	2.82	20.88
		IADPM	15.19%	2.06	21.44
		Our method	10.59%	1.90	23.21
	50%	FTVCS	12.04%	2.65	23.47
		IADPM	10.84%	2.14	24.61
		Our method	6.80%	1.91	27.01

the sampling rate, the SNR becomes higher and the relative error becomes lower for each method. Moreover, from Rerr and SNR of view, the superiority of our proposed method becomes more obvious. For example, when the level of sample ratio $SR = 50\%$ and the level of noise $\sigma = 0.1\%$, the SNR of Test image 1 adopting our proposed method is 26.66dB, while that produced by FTVCS and IADPM methods is 22.86dB and 23.68dB; the Rerr of Test image 1 obtained by our proposed method is 6.41%, while that produced by the other methods FTVCS and IADPM is 11.41% and 10.32%.

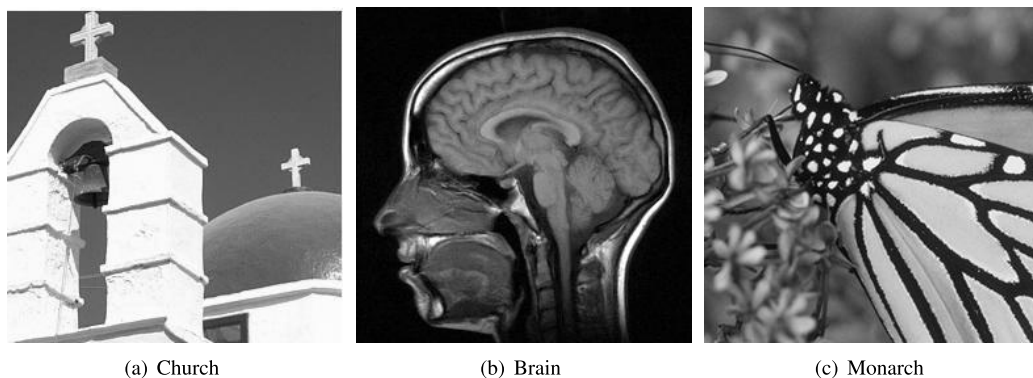


FIGURE 5. Test images.

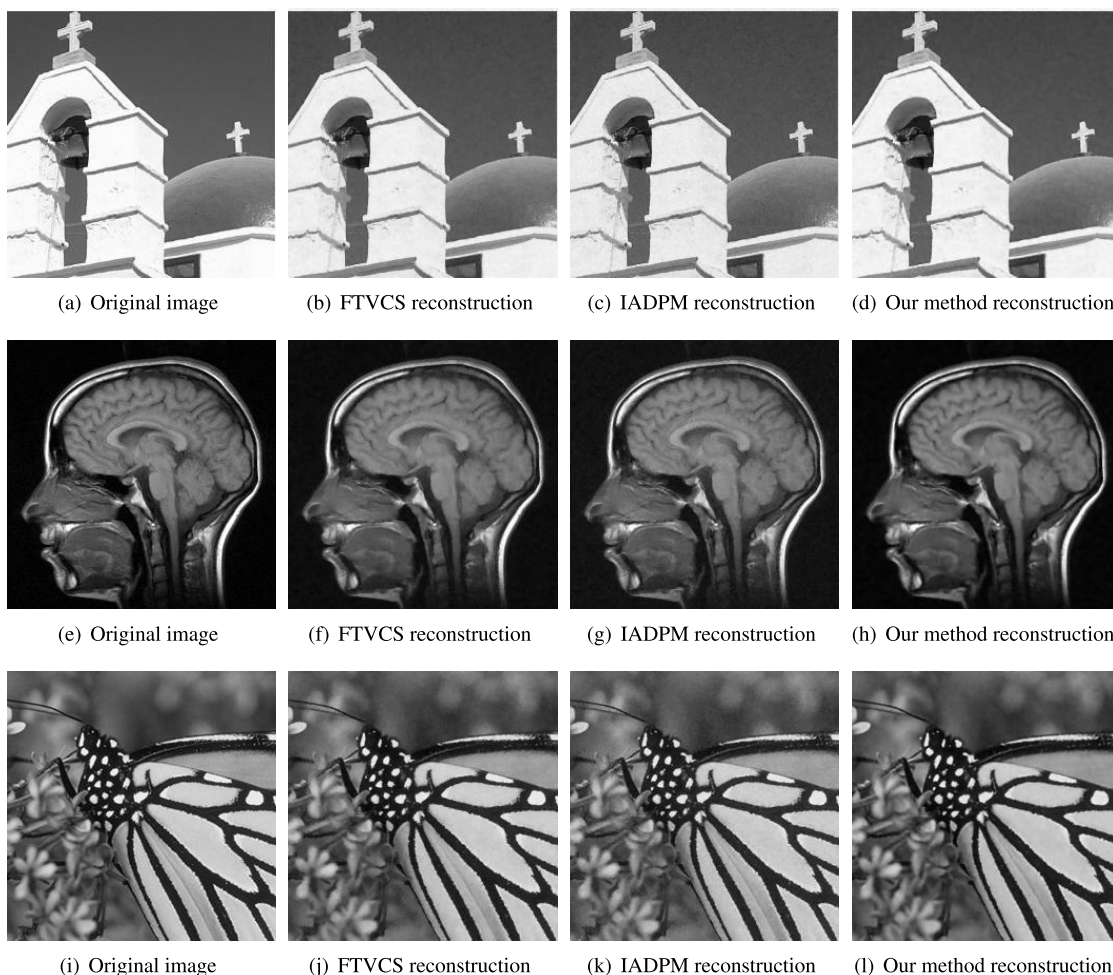


FIGURE 6. Experimental results from different reconstruction algorithms for the three sets of test images.

B. EXPERIMENT 2

In this experiment, we use partial cosine transform (DCT) matrix as CS encoder. Since the DCT matrix is implicitly stored as fast transforms for matrix vector multiplication, this enables us to test much larger images than Gaussian matrices. In this test, we use Church (256 × 256), Brain (256 × 256), and Monarch (256 × 256) as the test images. These three original images are displayed in Fig. 5. We randomly selected

50% DCT coefficients and added Gaussian noise of mean zero and standard deviation $\sigma = 1\%$. Experimental results on the three sets of test images, are shown in Fig. 6. It is clear from Fig. 6 that the reconstructed images of our method have more detailed information and are much closer to the original images as compared with the IADPM, FTVCS algorithms. For further comparison, two evaluation measures, the SNR (dB) and Rerr(%), are used to measure the performance of

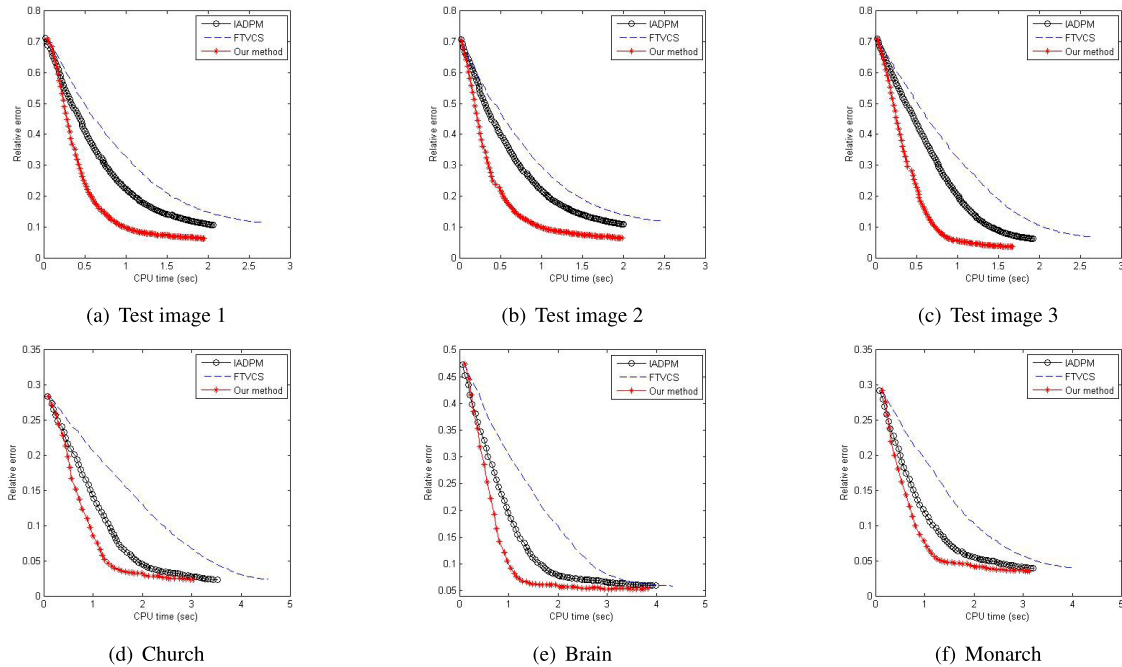


FIGURE 7. Relative errors versus CPU time for FTVCs, IADPM and our proposed method on six different test images (with SR=50%, $\sigma = 1\%$).

TABLE 3. The reconstructed results by Our method, FTVCs [16] and IADPM [22] for Test image 3.

Noise Level	SR	Method	Rerr(%)	Time(s)	SNR(dB)
$\sigma = 0.1\%$	30%	FTVCs	13.83%	2.96	20.46
		IADPM	13.16%	1.78	20.53
		Our method	9.19%	1.81	21.80
	40%	FTVCs	10.53%	2.89	22.69
		IADPM	9.82%	1.86	23.21
		Our method	6.11%	1.70	25.37
	50%	FTVCs	6.81%	2.82	25.48
		IADPM	6.07%	2.15	26.78
		Our method	3.69%	1.62	29.76
$\sigma = 1\%$	30%	FTVCs	13.89%	3.24	20.55
		IADPM	13.28%	1.67	20.56
		Our method	9.30%	1.78	21.71
	40%	FTVCs	10.57%	2.95	22.72
		IADPM	9.84%	1.90	23.24
		Our method	6.23%	1.68	25.21
	50%	FTVCs	6.92%	2.85	25.35
		IADPM	6.18%	2.07	26.66
		Our method	3.83%	1.62	29.52

our method for the three test images. Table 4 gives the SNR and Rerr of the reconstructed images resulting from the Our method, IADPM, and FTVCs methods. In general, these algorithms provide very good performance. Moreover, our proposed method outperforms FTVCs and IADPM in terms of the SNR and Rerr.

C. EXPERIMENT 3

To visibly show that the convergence results of FTVCs, IADPM and the proposed method for six different images, we plot six figures to illustrate the convergence performance of three tested methods from relative errors to CPU time,

TABLE 4. The SNR (dB) and Rerr(%) of three different methods for Church, Brain and Monarch.

Test images	Evaluation measures	FTVCs	IADPM	Our method
Church	Rerr(%)	2.43%	2.38%	2.32%
	SNR(dB)	32.26	32.47	32.69
Brain	Rerr(%)	5.96%	5.88%	5.37%
	SNR(dB)	24.43	24.56	25.36
Monarch	Rerr(%)	4.03%	3.96%	3.52%
	SNR(dB)	27.86	28.02	29.06

which are given in Fig. 7. As is clearly shown in Fig. 7, the relative errors of our proposed method is consistently lower than the other two methods. These facts also indicate that the proposed method performs better than FTVCs and IADPM.

REFERENCES

- [1] D. L. Donoho, "Compressed sensing," *IEEE Trans. Inf. Theory*, vol. 52, no. 4, pp. 1289–1306, Apr. 2006.
- [2] E. J. Candès, J. K. Romberg, and T. Tao, "Stable signal recovery from incomplete and inaccurate measurements," *Commun. Pure Appl. Math.*, vol. 59, no. 8, pp. 1207–1223, 2006.
- [3] J. Romberg, "Imaging via compressive sampling," *IEEE Signal Process. Mag.*, vol. 25, no. 2, pp. 14–20, Mar. 2008.
- [4] E. J. Candès, "The restricted isometry property and its implications for compressed sensing," *Comp. Rendus Math.*, vol. 346, nos. 9–10, pp. 589–592, May 2008.
- [5] H. Shen, X. Li, L. Zhang, D. Tao, and C. Zeng, "Compressed sensing-based inpainting of aqua moderate resolution imaging spectroradiometer band 6 using adaptive spectrum-weighted sparse Bayesian dictionary learning," *IEEE Trans. Geosci. Remote Sens.*, vol. 52, no. 2, pp. 894–906, Feb. 2014.
- [6] M. Lustig, D. L. Donoho, J. M. Santos, and J. M. Pauly, "Compressed sensing MRI," *IEEE Signal Process. Mag.*, vol. 25, no. 2, pp. 72–82, Mar. 2008.
- [7] J. Zhu, K. Li, and B. Hao, "Restoration of remote sensing images based on nonconvex constrained high-order total variation regularization," *Proc. SPIE*, vol. 13, no. 2, Jan. 2019, Art. no. 022006.

- [8] L. I. Rudin, S. Osher, and E. Fatemi, "Nonlinear total variation based noise removal algorithms," *Phys. D, Nonlinear Phenomena*, vol. 60, nos. 1–4, pp. 259–268, 1992.
- [9] G. Yu, L. Qi, and Y. Dai, "On nonmonotone chambolle gradient projection algorithms for total variation image restoration," *J. Math. Imag. Vis.*, vol. 35, no. 2, pp. 143–154, Oct. 2009.
- [10] B. Hao and J. Zhu, "Fast L_1 regularized iterative forward backward splitting with adaptive parameter selection for image restoration," *J. Vis. Commun. Image Represent.*, vol. 44, pp. 139–147, Apr. 2017.
- [11] J. Zhu, K. Li, and B. Hao, "Hybrid variational model based on alternating direction method for image restoration," *Adv. Difference Equ.*, vol. 2019, Jan. 2019, Art. no. 34.
- [12] J. Yu, M. Li, Y. Wang, and G. He, "A decomposition method for large-scale box constrained optimization," *Appl. Math. Comput.*, vol. 231, pp. 9–15, Mar. 2014.
- [13] J. Zhu and B. Hao, "A new smoothing method for solving nonlinear complementarity problems," *Open Math.*, vol. 17, no. 1, pp. 104–119, Mar. 2019.
- [14] Y. Wang, J. Yang, W. Yin, and Y. Zhang, "A new alternating minimization algorithm for total variation image reconstruction," *SIAM J. Imag. Sci.*, vol. 1, no. 3, pp. 248–272, Aug. 2008.
- [15] R. Y. Zhang, F. F. Xu, and J. C. Huang, "Reconstructing local volatility using total variation," *Acta Math. Sinica, English Ser.*, vol. 33, no. 2, pp. 263–277, Feb. 2017.
- [16] Y. Xiao, J. Yang, and X. Yuan, "Alternating algorithms for total variation image reconstruction from random projections," *Inverse Problems Imag.*, vol. 6, no. 3, pp. 547–563, 2012.
- [17] B. He, L.-Z. Liao, D. Han, and H. Yang, "A new inexact alternating directions method for monotone variational inequalities," *Math. Program.*, vol. 92, no. 1, pp. 103–118, 2002.
- [18] W. Shi, Q. Ling, K. Yuan, G. Wu, and W. Yin, "On the Linear Convergence of the ADMM in decentralized consensus optimization," *IEEE Trans. Signal Process.*, vol. 62, no. 7, pp. 1750–1761, Apr. 2014.
- [19] H. Li and Z. Lin, "Accelerated alternating direction method of multipliers: An optimal $O(1/K)$ nonergodic analysis," *J. Sci. Comput.*, vol. 79, no. 2, pp. 671–699, May 2019.
- [20] X. Li, H. Shen, H. Li, and L. Zhang, "Patch matching-based multitemporal group sparse representation for the missing information reconstruction of remote-sensing images," *IEEE J. Sel. Topics Appl. Earth Observ. Remote Sens.*, vol. 9, no. 8, pp. 3629–3641, Mar. 2016.
- [21] J. Yang and Y. Zhang, "Alternating direction algorithm for l_1 problems in compressed sensing," *SIAM J. Sci. Comput.*, vol. 33, no. 1, pp. 250–278, 2011.
- [22] J. Xu, Y. Qiao, Z. Fu, and Q. Wen, "Image block compressive sensing reconstruction via group-based sparse representation and nonlocal total variation," *Circuits Syst. Signal Process.*, vol. 38, no. 1, pp. 304–328, Jan. 2019.
- [23] Y.-H. Xiao and H.-N. Song, "An inexact alternating directions algorithm for constrained total variation regularized compressive sensing problems," *J. Math. Imag. Vis.*, vol. 44, no. 2, pp. 114–127, Oct. 2012.
- [24] S. Osher, Y. Mao, B. Dong, and W. Yin, "Fast linearized bregman iteration for compressed sensing and sparse denoising," *Commun. Math. Sci.*, vol. 8, no. 1, pp. 93–111, 2010.
- [25] M. A. T. Figueiredo, R. D. Nowak, and S. J. Wright, "Gradient projection for sparse reconstruction: Application to compressed sensing and other inverse problems," *IEEE J. Sel. Topics Signal Process.*, vol. 1, no. 4, pp. 586–597, Dec. 2007.
- [26] M. V. Afonso, J. M. Bioucas-Dias, and M. A. T. Figueiredo, "An augmented Lagrangian approach to the constrained optimization formulation of imaging inverse problems," *IEEE Trans. Image Process.*, vol. 20, no. 3, pp. 681–695, Mar. 2011.
- [27] G. Liu, T. Z. Huang, and J. Liu, "High-order TVL1-based images restoration and spatially adapted regularization parameter selection," *Comput. Math. Appl.*, vol. 67, no. 10, pp. 2015–2026, Jun. 2014.
- [28] J. G. Zhu, K. Li, and B. B. Hao, "Image restoration by second-order total generalized variation and wavelet frame regularization," *Complexity*, vol. 2019, Mar. 2019, Art. no. 3650128.
- [29] M. Lysaker and X.-C. Tai, "Iterative image restoration combining total variation minimization and a second-order functional," *Int. J. Comput. Vis.*, vol. 66, no. 1, pp. 5–18, 2006.
- [30] F. Li, C. Shen, J. Fan, and C. Shen, "Image restoration combining a total variational filter and a fourth-order filter," *J. Vis. Commun. Image Represent.*, vol. 18, no. 4, pp. 322–330, 2007.
- [31] X.-G. Lv, Y.-Z. Song, S.-X. Wang, and J. Le, "Image restoration with a high-order total variation minimization method," *Appl. Math. Model.*, vol. 37, nos. 16–17, pp. 8210–8224, Sep. 2013.
- [32] D. Krishnan, Q. V. Pham, and A. M. Yip, "A primal-dual active-set algorithm for bilaterally constrained total variation deblurring and piecewise constant Mumford-Shah segmentation problems," *Adv. Comput. Math.*, vol. 31, no. 1, pp. 237–266, Oct. 2009.
- [33] R. H. Chan, M. Tao, and X. Yuan, "Constrained total variation deblurring models and fast algorithms based on alternating direction method of multipliers," *SIAM J. Imag. Sci.*, vol. 6, no. 1, pp. 680–697, 2013.
- [34] M. Li, X. Kao, and H. Che, "Relaxed inertial accelerated algorithms for solving split equality feasibility problem," *J. Nonlinear Sci. Appl.*, vol. 10, no. 8, pp. 4109–4121, Jan. 2017.
- [35] L. Sun, G. He, Y. Wang, and C. Zhou, "An accurate active set Newton algorithm for large scale bound constrained optimization," *Appl. Math.*, vol. 56, no. 3, pp. 297–314, Jun. 2011.
- [36] F. Zheng, C. Han, and Y. Wang, "Parallel SSLE algorithm for large scale constrained optimization," *Appl. Math. Comput.*, vol. 217, no. 12, pp. 5377–5384, Feb. 2011.
- [37] Z. L. Tian, M. Tian, C. Gu, and X. Hao, "An accelerated Jacobi-gradient based iterative algorithm for solving Sylvester matrix equations," *Filomat*, vol. 31, no. 8, pp. 2381–2390, Jan. 2017.
- [38] A. Beck and M. Teboulle, "Fast gradient-based algorithms for constrained total variation image denoising and deblurring problems," *IEEE Trans. Image Process.*, vol. 18, no. 11, pp. 2419–2434, Nov. 2009.



BINBIN HAO received the Ph.D. degree in applied mathematics from Xidian University, Xi'an, China, in 2010. She joined the College of Science, China University of Petroleum, in 2009, and has been an Associate Professor, since 2012. Her current research interests include image processing, pattern recognition, wavelet analysis, and sparse representation.



JICHAO WANG was born in 1979. He received the Ph.D. degree from the Institute of Oceanology, Chinese Academy of Sciences. His current research interests include stochastic differential equations, dynamic systems, and data assimilation.



JIANGUANG ZHU received the Ph.D. degree in applied mathematics from Xidian University, Xi'an, China, in 2011. He is currently an Associate Professor with the Shandong University of Science and Technology. His current research interests include optimization theory, algorithms and applications in image processing, and sparse representation.

• • •